SCOPE | SAUDI INTERNATIONAL CONFERENCE ON NUCLEAR POWER ENGINEERING

Proceedings of SCOPE
13-15 Nov. 2023 – KFUPM
Paper 23023

Experimental PIV Measurements in a Randomly Packed Isothermal Pebble Bed Core Prototype

Abdulaziz Almathami
Department of Nuclear Engineering,
Thermal Hydraulics Research Laboratory,
Texas A&M University, College Station, TX – 77845.
almathaa@tamu.edu:

Blake R. Maher
J. Mike Walker '66 Department of Mechanical Engineering,
Thermal Hydraulics Research Laboratory,
Texas A&M University, College Station, TX – 77845.
brmaher27@tamu.edu;

Yassin A. Hassan
Department of Nuclear Engineering,
J. Mike Walker '66 Department of Mechanical Engineering,
Thermal Hydraulics Research Laboratory
Texas A&M University, College Station, TX – 77845.
y-hassan@tamu.edu

Abstract – *Pebble Bed Reactors (PBR) are a Generation-IV reactor design which are a subject of extensive research – due to their increased mixing and turbulence characteristics. Packed beds have sophisticated yet randomized geometry with vacant spaces, increasing the flow complexity in PBR cores. This experimental research on a facility of randomly packed pebble bed spheres investigates the complex flow phenomena within a PBR core to simulate fluid dynamics. By utilizing Particle Image Velocimetry (PIV) on the near-wall boundary and among the spheres, high-fidelity velocity measurements were carried out. In this facility, Matched Index of Refraction (MIR) provides a clear view of the packed spheres to analyze the flow at microscopic scales with precise resolution. The flow was investigated for various Reynolds numbers (Re) by utilizing PIV measurements. In order to provide a comprehensive profile of the flow and geometry that was studied, a three-dimensional reconstruction of the flow was carried out. This serves the primary purpose of providing the geometry for validation of simulation as well as the secondary purpose of illustrating the geometry of the packed bed. The experiments investigated isothermal and non-isothermal conditions to examine the differences in flow dynamic patterns within packed spheres. The results characterize first- and second-order flow statistics including instantaneous velocity magnitude, mean velocity, velocity fluctuations, and Reynolds stresses. Moreover, the effect of different Reynolds number boundaries and spheres were investigated. Increasing Reynolds numbers (Re) was observed to affect the fluid dynamics within the pebble bed geometry, highlighting an increase in turbulence and flow mixing between spheres and within the gaps. This experimental campaign provides unique high-fidelity data sets for computational fluid dynamics model development and validation.*

Keywords: *Randomly Packed Spheres, Pebble Bed, Experimental, PIV*

I. Introduction

The investigation of fluid flow over spheres is a commonly investigated topic in fluid mechanics. The random nature of the packed bed geometry leads to complex flow patterns which are of great interest in simulation, validation, and experimentation. Complex flow characteristics such as change in preferential flow path with Reynolds number,

stagnation regions leading to hot spotting in fuel elements, and varying development length dependent on local porosity are important to investigate [1]. Complex flow such as this is caused by a variety of phenomena such as vortex shedding, shear layer instability, and flow separation [2]. This study focuses on reactors utilizing pebble bed fuel elements in nuclear power reactors such as high temperature gas cooled reactor (HTGR) [2]. The geometry of this study depends on evaluation and validation of previous experimental and computational studies [2-4].

Matched-Index-of-Refraction (MIR) is a technique that is widely used to obtain a clear view of the interior of optically opaque geometries and reduce optical distortion that occurs when light passes through two materials with different refractive indices. This is accomplished by selecting the refractive index of the fluid so that it matches the solid material's refractive index [5]. Utilizing MIR techniques in the capturing of images serves to enhance image clarity and thereby facilitates a more thorough characterization of the flow phenomena and complexities present in current experiment output.
The data were collected across two distinct conditions, isothermal, and were applied to two stainless steel spheres for varying Reynolds numbers (Re). The flow phenomena were measured using Particle Image Velocimetry (PIV). The experimental study was conducted at two different Reynolds numbers, forced convection (Re = 159 & Re = 1710) regimes. The results of the experiment provide a comprehensive high-fidelity data set for computational model validation.

II. Experimental Facility and Methodology

This section describes the setup and equipment used for the experiments, including the facility, instruments, and conditions under which the experiments were conducted. The specific instruments mentioned are PIV equipment is also shown in Fig. 1. The primary flow system consisted of a fluid channel, flexible piping, and surge tank. The flow was monitored by a Coriolis flow meter and controlled by a centrifugal pump connected to Variable Frequency Drive (VFD). The system also included a large tank for storing D-Limonene [6]. The test section employed in this study was comprised of a circular borosilicate glass duct filled with randomly packed acrylic and glass spheres with a diameter of 30 mm. Also included were two stainless steel spheres with a diameter of 30 mm. The test section was supported by an aluminum structure, and included a correction box. This correction box is used to reduce optical distortion stemming from viewing a liquid through a curved surface. The stainless-steel spheres were placed vertically and close to the test section as shown in Fig. 2. The test was isothermal, with fluid injected to the section through a development region and passing through a flow straightener, flowing toward the top of the test section. When the flow was confirmed to have reached a steady state, images were captured by PIV instrumentation.

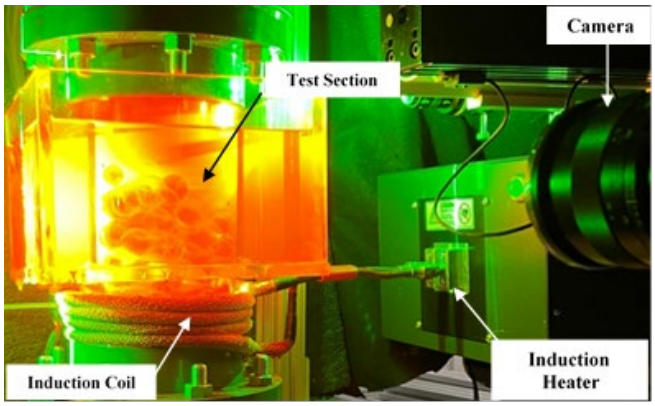

Fig. 1. Overview of the facility test section.

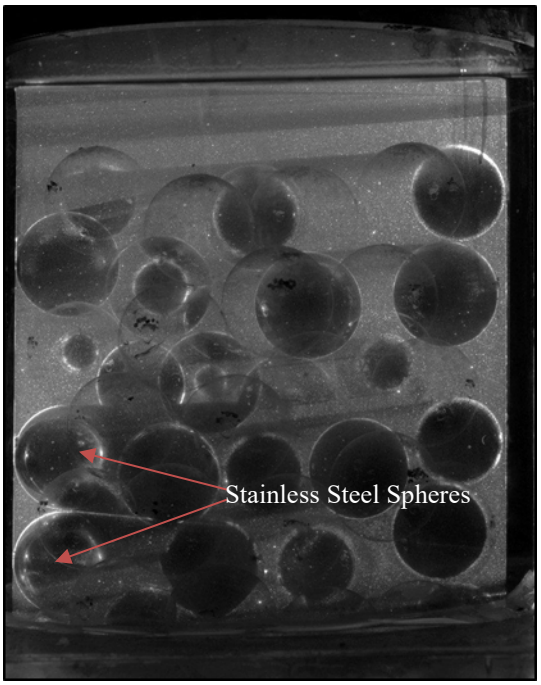

Fig. 2. Overview of the facility test section showing stainless steel spheres position

The lasers used for carrying out the PIV measurement were also employed in the three-dimensional scanning of the bed. The lasers were perfectly aligned with one another and the camera focused, then both lasers and the camera were moved in a synchronized manner in the direction of the camera view. The first captured image was at the wall of the duct nearest to the camera and the final image was at the wall furthest from the camera. The images captured during this procedure were then processed and the centers of all of

the spheres within the bed were located. The centers of the spheres were plotted and converted to a common computer aided design (CAD) file which can be used to recreate the exact geometry used in this experiment in simulations. This addresses a common problem associated with the random nature of pebble bed packing which is that it is difficult to compare experimental and simulation results on different randomly packed geometries. An image of the CAD file is displayed in Fig. 3.

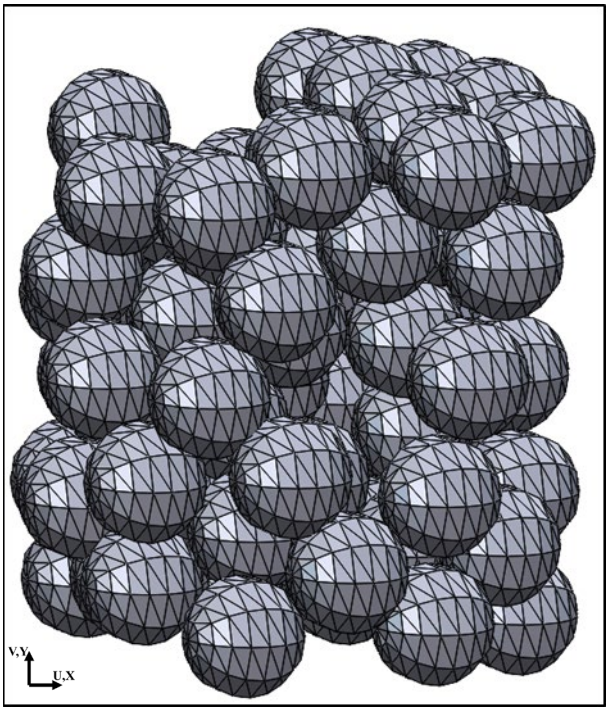

Fig. 3. CAD file of randomly packed bed reconstruction

III. Data Analysis

A combination of custom-developed code and open-source image processing software was used to process the data. The approach is similar to the methods outlined in previous studies [3, 7]. The raw video files were converted into velocity vectors, and then a custom code was used to generate results images.

III.A. Particle Image Velocimetry (PIV)

Particle Image Velocimetry is a technique that uses images from a video to determine the velocity of particles in a flow. This method analyzes raw captured image files to generate velocity vectors of the particles. It has been employed in a wide range of pebble bed flow visualization studies [2,8]. The technique analyzes the frames of the raw video files to track the movement of the seeding particles (in this case, silver coated glass spheres) from one frame to the next, generating velocities in terms of pixels displaced per time between frames. Using spatial calibration, these velocities are then converted to meters per second. The process of tracking the particles is carried out using a robust phase correlation method with multi-grid multi-pass techniques and overlapping windows with a first pass window of size 64x64 and second and third pass window size of 32x32 pixels [3,9]. Statistical validation techniques to ensure accuracy of the results include using a 50% overlap between passes and applying a median filter to eliminate any false velocity vectors. The resulting blank spaces are then filled by using interpolated values [10].

IV. Results

In this section, the relevant flow statistics of the measured velocity fields are presented and discussed. The primary focus of this presentation and discussion is to provide an overview of the measurements performed as they relate to common validation metrics. The data obtained from two separate runs per Reynolds number allowed for a thorough analysis of the flow characteristics. The velocity magnitude, mean velocity, RMS velocity fluctuations, and vorticity were calculated to gain a better understanding of the flow behavior

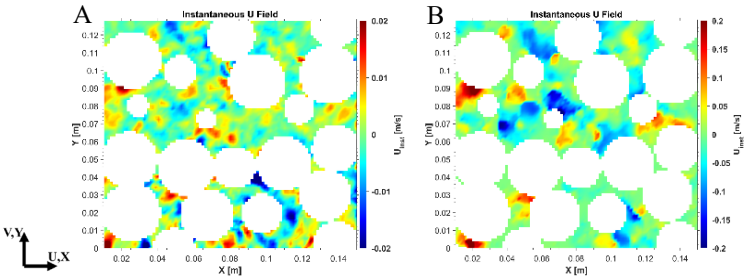

Fig. 4. Instantaneous Velocity of U Components A) Re = 1710, B) 159 respectively

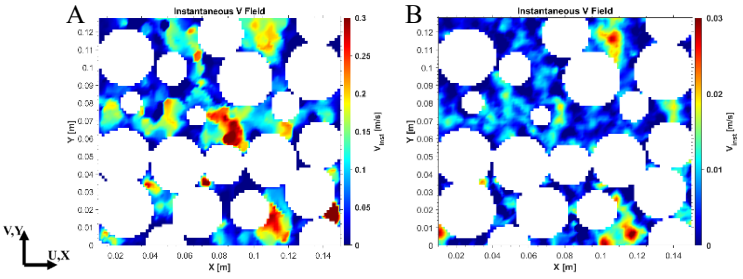

Fig. 5. Instantaneous Velocity of V Components A) Re = 1710, B) 159 respectively

In the figures in question, the instantaneous velocity vector fields for U and V components are shown for two different

Reynolds numbers. By examining these fields, it becomes clear that as the Reynolds number increases, the flow patterns become more complex and turbulent, leading to an increased mixing of fluid in the packed spheres. The overlay of the velocity vectors and flow contours on the resulting images improves the visual representation of the flow inside the test section. The flow patterns can be seen more clearly, providing a better understanding of the fluid dynamics present in the system. The instantaneous velocity vector fields in Fig. 4 and 5 provide valuable information about the fluid dynamics in the voids between the packed spheres and the impact of Reynolds number on the observed behavior. The fluid velocity was faster in the Re = 1710 case for both velocity components, leading to increased fluid flow and increased preference of the flow toward the wall boundaries [11]. The velocity contour maps can aid in the understanding of the flow patterns, making them useful for the validation of simulations used for the design and optimization of pebble bed cores.

Figures 6, 7 provide visual representation of the mean velocity vector for U and V components at different Reynolds numbers. The magnitude of the mean velocity increases as the Reynolds number increases, indicating the dominance of inertial forces over viscous forces at higher Reynolds numbers. Some smoothing of the flow behavior demonstrated in the instantaneous velocity measurements occurs as would be expected, but the general trend of increased velocity at the wall boundary as well as recirculation and wake variance toward the test section outlet continues to be visible.

The bypass flow close to the wall has a noticeable effect on the velocity field, as seen in the area above the two stainless steel spheres in the figures. The bypass flow is a result of the increased local porosity of the randomly packed bed near the wall. While some bypass flow exists at all Reynolds numbers observed, the proportion of flow near the wall increases as the Reynolds number increases. The direct physical cause of this phenomena is increased local friction factor at the lower porosity regions of the bed. The total porosity was estimated as per Eqn. (1) shown below, as per Du Toit and Rosslee [12].

$$\varepsilon_b = 1 - \frac{V_S}{V_T} \qquad (1)$$

Where, ε_b is the estimated total radial porosity and V_S the volume covered by the spheres and V_T is the total volume. The total porosity was calculated as 0.477.

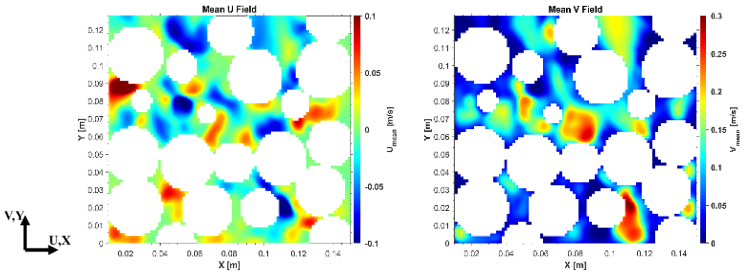

Fig. 6. Mean Velocity Fields of Re = 1710

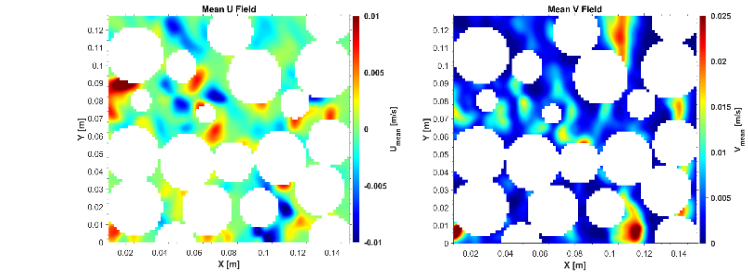

Fig. 7. Mean Velocity Fields of Re = 159

The contours of the RMS velocity fluctuations in the figures show the variation in turbulence intensity at different Reynolds numbers. Fig. 8 and 9 indicate that turbulent intensity increases with increasing Reynolds number. This is because higher Reynolds numbers led to more turbulent fluctuation. Therefore, higher fluctuation would occur above the spheres due to the increased chaotic dynamic pressure distribution within the bed. The difference between horizontal and vertical components becomes more pronounced as Reynolds number increases, showing a proportional reduction in the horizontal fluctuation as the flow is driven with greater motivation along the axial direction.

At Reynolds number 159, fluctuation is observed to be higher near the wall compared to the other test, which could be due to the wall boundary layer and larger void regions which allow for increased fluid movement. At Reynolds number 1710, the highest turbulent intensity is seen, with more complex and intense turbulence structures. Upon close examination of Fig. 8, it is observed that the top area (near duct exit) exhibits high fluctuations. This is due to a more intense wake structure within the flow upon exiting the packed bed. In contrast, the flow in the other case was at a lower velocity, leading to a smoother flow with less wake fluctuation. Fig. 9 shows the effect of viscous forces are more pronounced for Re=159 compared to Re=1710.

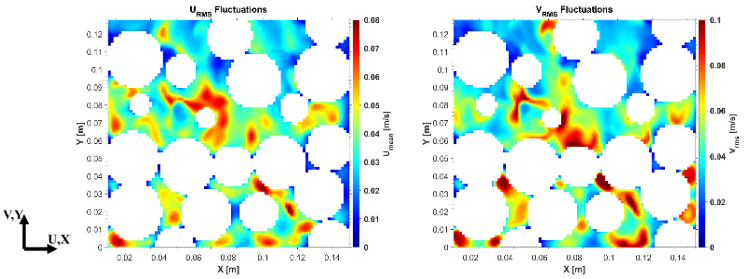

Fig.8. Root-Mean-Square Fluctuations of the horizontal and vertical velocity components (u′ and v′) for Re = 1710

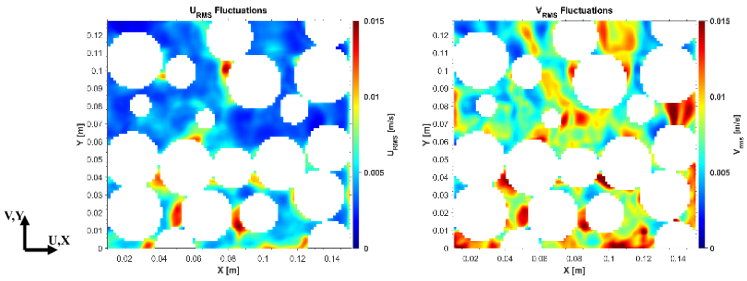

Fig.9. Root-Mean-Square Fluctuations of the horizontal and vertical velocity components (u′ and v′) for Re = 159

In Fig. 10 can be seen that the negative and positive values of u′ v′ in the color maps indicate the presence of shear layers. The magnitude of these values increases with higher Reynolds numbers. As the Reynolds number increases, fluid boundary instabilities occur and the fluid shear increases, leading to higher turbulence.

It is important to note that the complexity of the flow close to the wall increases with higher Reynolds numbers, as indicated in the figure 10. Furthermore, the bed exit region of the contours in Fig. 10 displays higher Reynolds stress as a result of turbulent flow when the fluid passes the spheres at high velocity. As the velocity fluctuation decreases, the Reynolds stress also reduces.

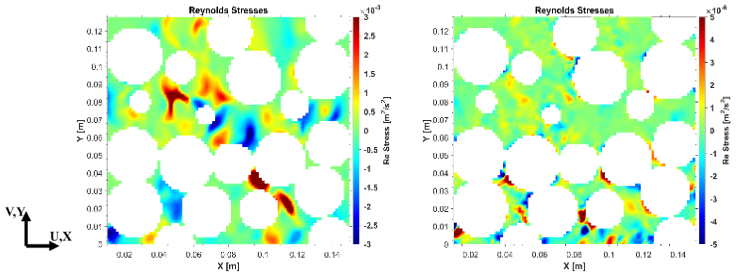

Fig. 10. Reynolds Stress for Re = 1710, 159 respectively

Vorticity is an important factor in packed bed systems, which can greatly affect the behavior of the fluid and its ability to mix and transport heat and mass.

In Fig 11, vorticity is shown in the test section with negative values indicating fluid rotating in a clockwise direction and positive values indicating fluid rotating in a counter-clockwise direction. The figure demonstrates the significance of vorticity in fluid flow systems, as the increase in Reynolds number leads to an increase in the complexity of vorticity.

The increase in vorticity complexity can lead to more intense turbulence and fluid mixing, which can result in greater momentum transfer rates. In addition, vorticity can influence the formation of eddies within the fluid, which can impact the overall flow patterns and stability of the system. The results of this analysis will provide valuable insights for engineers and researchers looking to optimize the performance of packed sphere systems in a wide range of industrial applications through the use of well-validated simulation.

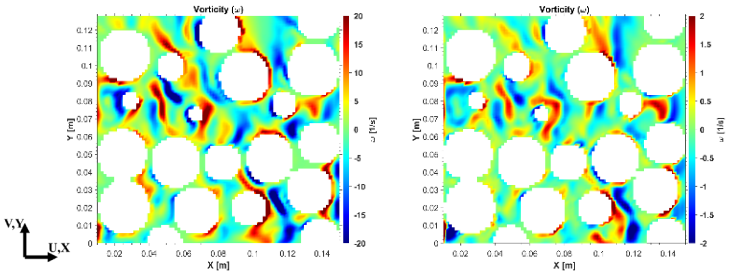

Fig. 11. Vorticity for Re = 1710, 159 respectively

IV. Conclusions

Particle Image Velocimetry measurements were carried out on a randomly packed bed geometry employing a matched index of refraction construction. The geometry was three dimensionally scanned in order to provide the geometry for simulation and direct comparison. The measurements that were carried out were analyzed and discussed in order to better understand the effects of change in Reynolds number (Re = 1710, 159) on an isothermal packed bed.

The random nature of the bed was consistent for all but two stainless steel spheres, which were deliberately placed near the wall at the centerline of the packed bed in order to study the effects in the near wall region and the relationship this has with the expected variance in flow in the bypass region of a packed bed. The changes in behavior of the flow aligned with the generally accepted norms of pebble bed velocity analysis but contributed the vital additional analysis of the effects of stainless-steel spheres. This additional measurement is a valuable contribution to the community as fluid mechanics modeling is a critical aspect of simulation that requires rich experimental data for validation. This study seeks to provide that validation data and the results demonstrated within serve as execution of this objective.

References

1. C.G. DU Toit, "Radial variation in porosity in annular packed beds*" Nuclear Engineering and Design* **238** (2007).
2. R. Muyshondt et al., "Flow and heat transfer in the wake of a triangular arrangement of spheres," *Physics of Fluids* **33** 11 (2021).
3. T. Nguyen et al., "Experimental investigation of cross flow mixing in a randomly packed bed and streamwise vortex characteristics using particle image velocimetry and proper orthogonal decomposition analysis," *Physics of Fluids* **31** 2 (2019).
4. T. NGUYEN, "PIV measurements of turbulent flows in a 61-pin wire-wrapped hexagonal fuel bundle," *International Journal of Heat and Fluid Flow* **140**, 47 (2017).
5. Noushin Amini and Yassin A. Hassan, "An investigation of matched index of refraction technique and its application in optical measurements of fluid flow," *Experiments in Fluids* **53** (2020).
6. M. K. V. Pandi Anand Akumar, Sattu Kamaraj, "D-limonene: A multifunctional compound with potent therapeutic effects," *Journal of Food Biochemistry* **45** 1 (2020).
7. D. Orea et al., "Experimental measurements of flow mixing in cold leg of a pressurized water reactor," *Annals of Nuclear Energy* **140**, 107137 (2020).
8. Y. Takatsu and T. Masuoka, "Transition Process to Turbulent Flow in Porous Media," *International Mechanical Engineering Congress and Exposition* **42223**, 573 (2005).
9. A. Eckstein and P. P. Vlachos, "Digital particle image velocimetry (DPIV) robust phase correlation," *Measurement Science and Technology* **20**, 055401 (2009).
10. J. Westerweel, "'Efficient detection of spurious vectors in particle image velocimetry data," *Experiments in fluids*, **16** 236–247 (1994).
11. J. K. Eato and J. R. Fessle, "Preferential Concentration of Particles by Turbulence," *Int. J. Multiphase Flow* **20**, 169 (1994).
12. C. G. Du Toit and P. J. Rosslee, "Analysis of the porous structure of packed beds of spheres using X-ray computed tomography," *8th South African Conference on Computational and Applied Mechanics, SACAM 2012* - Conference Proceedings January 2016, 31 (2012).